Characterisation of timber connection behaviour from reduced scaled experiments based on similitude laws

Yann Sousseau, Sidi Mohammed El Achachi, Myriam Chaplain, Carole Faye, Thomas Catterou, Patrice Garcia

WCTE 2020
WORLD CONFERENCE ON TIMBER ENGINEERING
SANTIAGO, CHILE | 24 - 27 AUGUST

CHARACTERISATION OF TIMBER CONNECTION BEHAVIOUR FROM REDUCED SCALED EXPERIMENTS BASED ON SIMILITUDE LAWS

Yann Sousseau[1], Sidi Mohammed Elachachi[1], Myriam Chaplain[1], Carole Faye[2], Thomas Catterou[2], Patrice Garcia[2]

ABSTRACT: Testing a full size structure requires very expensive means. Therefore, the proposed methodology consists in testing a representative scaled down model, whose design is based on similitude laws. The purpose of this article is the constitution, for timber construction, of scale factors related to mechanical characteristics of frame connections, for 1/2 and 1/3 reduced scales. Firstly, scale factors were obtained by experimental tests on connections and then compared to the theoretical ones. Discrepancies have been noticed between experimental and theoretical scale factors. For most connection characteristics, discrepancies not only result from dispersions noticed on the three scales, but also from distortions in connections geometry. Secondly, a numerical approach will be developed to predict the timber construction behaviour, whose input data are provided by mechanical characteristics, described in this paper.

KEYWORDS: Timber construction, Frame connections, Experiment, Similitude laws, Scaled model, Uncertainty

1 INTRODUCTION

To perform full size tests requires expensive means. A possible solution is to test a representative reduced size building, whose design is based on similitude laws [1]–[3]. Then, from observed responses on reduced scale, the similitude laws allow to deduce those in full scale (Figure 1). For that, scale factors have to be established. They are defined, for each x variable (parameters or variable of interest) as the ratio

$$\lambda_x = x^{(F)}/x^{(R)} \quad (1)$$

with $x^{(F)}$ and $x^{(R)}$ the values for x at (F) full scale and (R) reduced scale respectively. A set of values assigned to theses factor is a similitude law.

Similitude laws theory has been developed mainly in structures (automobile, aeronautics and aerospace) and fluid mechanics [1], [2]. Recently, some works have dealt with civil engineering structures [4], [5]. To constitute similitude laws, several methods in literature have been developed: Dimensional Analysis (DA) and Similitude Theory Applied to Governing Equations (STAGE). Based mainly on mathematical principles, these methods are usable for any ideal physical behaviour's study. Once the study's behaviour is defined, these methods result in similitude relationships, which are relationships between scale factors. Because of the number of equations superior to unknown scale factors, there are many potential similitude laws.

DA method [6]–[8] is used in structures [9]–[13] and fluid mechanics [14]–[17]. This method, which uses Vaschy-Buckingham theorem, does not require the knowledge of behaviour equations.

STAGE method [2], [3] is based on behaviour equations, which need to be established (but not necessarily to resolve). This method is based on conservation equations from reduced scale to full scale. Most authors using STAGE study behaviours which may be described by equations. For example, equation from thin plate theory is used to characterize steel plates vibrations behaviour in aeronautic [18]–[21]. Equation from composite structure behaviour are also used for wind turbine[3], [22]–[25]. Note that similitude laws reliability may be impacted if equations used do not take into account some influent phenomena [26], [27]. Finally, for some behaviour equations, STAGE makes accessible some similitude laws [28], [29] which are not with DA method.

For these works, similitude laws obtained with STAGE are same as those obtained with DA, so the latter will be used. Note that, in literature very little work focus on both timber and similitude laws.

[1] Yann Sousseau, university of Bordeaux, France, yann.sousseau@u-bordeaux.fr
Sidi-Mohammed Elachachi, university of Bordeaux, France, sidi-mohammed.elachachi@u-bordeaux.fr
Myriam Chaplain, university of Bordeaux, France, myriam.chaplain@u-bordeaux.fr

[2] Thomas Catterou, technologic institute FCBA, France, thomas.catterou@fcba.fr
Patrice Garcia, technologic institute FCBA, France, patrice.garcia@fcba.fr
Carole Faye, technologic institute FCBA, France, carole.faye@fcba.fr

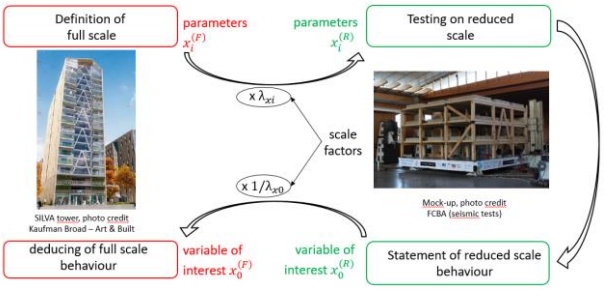

Figure 1: *Similitude laws principle*

These works are the first step of a research programme to establish similitude laws to study mid and high-rise timber buildings behaviour. The studied structure (Figure 2) is representative of constructive systems frequently used in mid and high-rise timber buildings.

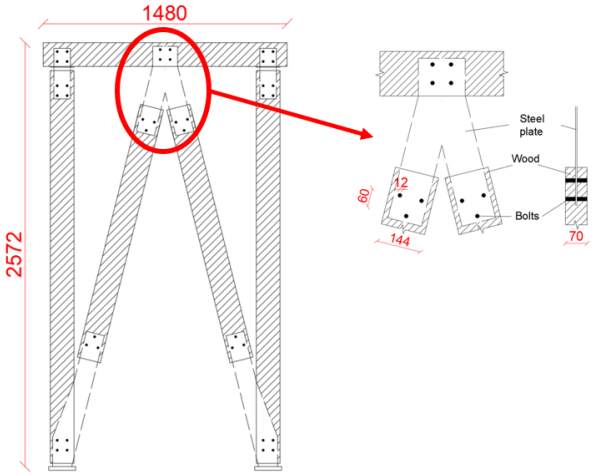

Figure 2: *Studied structure and joints*

This paper focuses in establishing a similitude law allowing to estimate the main connections mechanical characteristics: elastic stiffness K_e (N/m), strength F_u (N) and associated displacement u_u (m). The parameters, whose studied characteristics depend, and which need to be considered, are the material properties C (elasticity modulus, stress limits,… in N/m²) and the geometrical properties L (in m). Using DA, the similitude relationships are obtained as follows:

$$\begin{cases} [K_e] = [C][L] \\ [F_u] = [C][L]^2 \\ [u_u] = [L] \end{cases} \Rightarrow \begin{cases} \lambda_{Ke} = \lambda_C \lambda_L \\ \lambda_{Fu} = \lambda_C \lambda_L^2 \\ \lambda_{uu} = \lambda_L \end{cases} \quad (2)$$

where $[x]$ is the x unit and λ_x is the scale factor associated to x. In our study, specimens are, for full and reduced scale, made of the same materials. However, despite materials are same between full and reduced scale, material properties can be different. Indeed, it was observed in literature [30]–[32] variations of material properties with size reduction (for example, stress limits increase). Such phenomena are called material scale effects. Otherwise, these properties can be different between full and reduced scale, because of material properties variability. First, material scale effects and variability not being considered, so the best hypothesis for material properties is to take a scale factor (λ_c) equal to 1. Therefore, for 1/2 reduced scale, similitude law is $\lambda_{Ke} = 2$, $\lambda_{Fu} = 4$ and $\lambda_{uu} = 2$, and for 1/3 reduced scale, similitude law is $\lambda_{Ke} = 3$, $\lambda_{Fu} = 9$ and $\lambda_{uu} = 3$. However, because of technological reasons, reduction steel plate thickness e is hard to realize as the thickness is already small in full scale. Also, the factor λ_{a0} of the edge spacing a_0 (Figure 3) is not taken equal to λ_L, in order to avoid undesirable fracture by failure [33]–[35]. Such situations are called distortions. Therefore, the λ_{Ke}, λ_{Fu} and λ_{uu} experimental values may differ from those given by DA (equation (2)). Problematics of distortion are frequently raised in the literature, for example because of impossibility to reduce thin steel elements [18], [19], [36]. Therefore, the cited authors establish empirical similitude laws from numerical simulations.

First, connections are experimentally tested in full and reduced scales, in order to determine their characteristics. Then, the scale one behaviour is estimated from reduced scales experimental results and scale factors. Also, from full scale experimental results, the experimental scale factors are deduced, and are compared with the theoretical ones.

2 EXPERIMENTAL STUDY OF CONNECTIONS BEHAVIOUR

2.1 TESTS DESCRIPTION

The tested connections and test configuration are presented in Figure 3. The reduced scale connections dimensions are deduced from full scale ones and the scale factor λ_L.

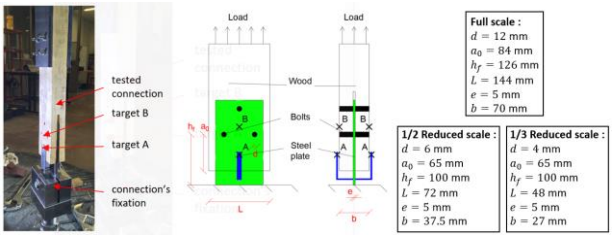

Figure 3: *Tested connections*

The tests are performed according to EN NF 26 891 standard [37]. The axial load is applied in tension or compression. The relative displacement between steel plate and wood (targets A and B respectively, Figure 3), the slide of the joint (u), is measured. Targets located on bolt edge sides allow measuring bolt deformation mode. These tests are monotone and under slide of the joint control. This displacement u evolves as follows (Figure 4): increase until load reaches $0.4F_{u,\text{th}}$ (A-B,

$F_{u,\mathrm{th}}$ is estimated theoretical strength), stabilization during 30 seconds (B-C), decrease until load reaches $0.1F_{u,\mathrm{th}}$ (C-D), stabilization during 30 seconds (D-E), increase until fracture (E-F). Without 2-3 et 4-5 steps, the displacement evolves with a constant rate.

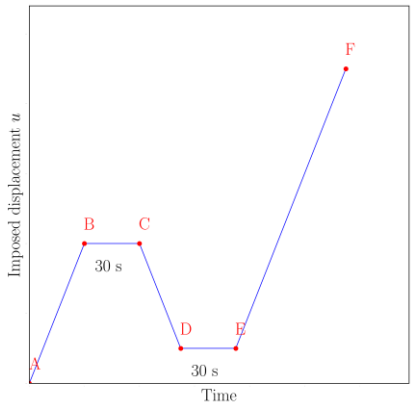

Figure 4: *Displacement, joint slide u, control during test*

2.2 MAIN CHARACTERISTICS DETERMINATION

For one test, the load displacement curve (Figure 5) is obtained, from which the mains characteristics are calculated: elastic stiffness K_e, strength F_u and associated displacement u_u. Stiffness K_e is obtained by linear regression, between the points corresponding to E-F step and for which $F < 0.4F_u$ [33], [34] (this corresponds to D0-D1 on Figure 5). Then (A-E) parts are removed from curve, which is shifted so that its extension passes through origin. Displacement u_u is determined from shifted curve. Also, points whose displacement is greater than u_u and force is lower than $0.9F_u$ are removed from the curve. The resulting maximum displacement of processed curve (Figure 5) is noted $u_{\max}$

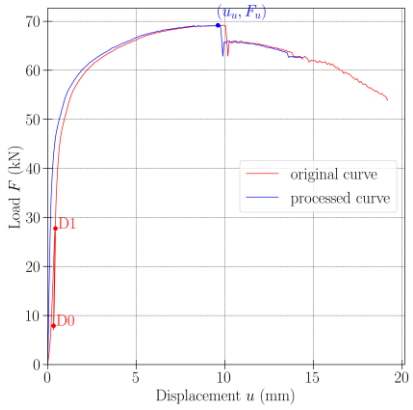

Figure 5: *Load displacement curve for one test in full scale*

For one test, a load displacement behaviour model is established. Saws model [38]–[40] is chosen for these works and is described by the equation (3) :

$$\begin{cases} u \le u_u : F = (F_0 + r_1 K_e u)\left(1 - \mathrm{e}^{-\frac{K_e u}{F_0}}\right) \\ u_u < u \le u_{\max} : F = F_u + r_2 K_e (u - u_u) \end{cases} \quad (3)$$

with u the displacement, F the load, and

$$F_u = (F_0 + r_1 K_e u_u)\left(1 - \mathrm{e}^{\frac{-K_e u_u}{F_0}}\right) \quad (4)$$

The negative slope $r_2 K_e$ is determined by linear regression between (u_u, F_u) and the end of the curve. The $f_0 = F_0/F_u$ coefficient is calculated by the mean square method between experimental F values and those given by equation (3).

Then, for one given scale, mean characteristic values (Tables 1, 2 and 3) are calculated based on all tests in tension and compression, from which a representative model curve is established (Figures 6, 7 and 8, black curve), based on equation (3). Dispersion is important, and it will be noticed later the significant impact on scale factors dispersion.

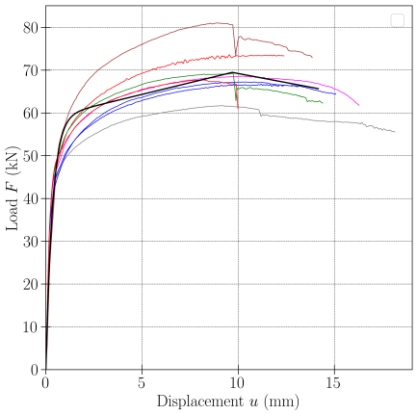

Figure 6: *Experimental load displacement curves (shifted) for all tests, full scale*

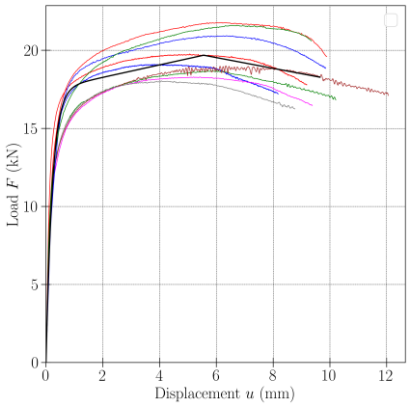

Figure 7: *Experimental load displacement curves (shifted) for all tests, 1/2 reduced scale*

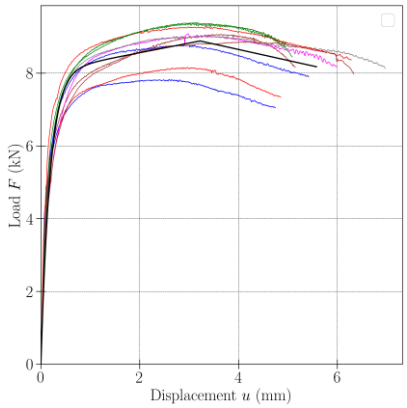

Figure 8: *Experimental load displacement curves (shifted) for all tests, 1/3 reduced scale*

Table 1: *Experimental characteristics, full scale*

Quantity of tests	$n^{(\mathrm{F})} = 8$	
Characteristic x	Experimental mean $\overline{x^{(\mathrm{F})}}$	COV (%)
Elastic stiffness K_e (MN/m)	174	18.5
Strength F_u (kN)	69.5	8.20
Displacement u_u (mm)	9.69	10.7
Coefficient f_0	0.847	1.42
Coefficient r_2	-0.0049	96
Displacement $u_{\max}$ (mm)	14.2	17.5

Table 2: *Experimental characteristics, 1/2 reduced scale*

Quantity of tests	$n^{(\mathrm{R})} = 9$	
Characteristic x	Experimental mean $\overline{x^{(\mathrm{R})}}$	COV (%)
Elastic stiffness K_e (MN/m)	79.7	17.2
Strength F_u (kN)	19.7	7.20
Displacement u_u (mm)	5.55	18.7
Coefficient f_0	0.887	3.77
Coefficient r_2	-0.0043	39
Displacement $u_{\max}$ (mm)	9.65	11.3

Table 3: *Experimental characteristics, 1/3 reduced scale*

Quantity of tests	$n^{(\mathrm{R})} = 10$	
Characteristic x	Experimental mean $\overline{x^{(\mathrm{R})}}$	COV (%)
Elastic stiffness K_e (MN/m)	44.2	19.3
Strength F_u (kN)	8.89	5.82
Displacement u_u (mm)	3.22	13.8
Coefficient f_0	0.904	2.34
Coefficient r_2	-0.0068	32
Displacement $u_{\max}$ (mm)	5.58	13.7

2.3 EVALUATION OF SIMILITUDE SCALE FACTORS

The experimental scale factors are obtained using equation (1), for each x studied characteristic, then are compared with the theoretical ones $\lambda_x^{(\mathrm{th})}$ (Tables 4 and 5). The experimental mean value for λ_x, $\overline{\lambda_x}$, is so obtained by

$$\overline{\lambda_x} = \overline{x^{(\mathrm{F})}} / \overline{x^{(\mathrm{R})}} \tag{5}$$

and its standard deviation, σ_{λ_x} by

$$\left(\sigma_{\lambda_x}\right)^2 = \left(\frac{\sigma_{x^{(\mathrm{F})}}}{\overline{x^{(\mathrm{R})}}}\right)^2 + \left(\sigma_{x^{(\mathrm{R})}} \frac{\overline{x^{(\mathrm{F})}}}{\left(\overline{x^{(\mathrm{R})}}\right)^2}\right)^2 \tag{6}$$

Table 4: *Comparison between experimental and theoretical scale factors, for 1/2 scale*

Characteristic x	Theoretical scale factor $\lambda_x^{(\mathrm{th})}$	Experimental scale factor λ_x	
		Experimental mean $\overline{\lambda_x}$	COV (%)
Elastic stiffness K_e (N/m)	2	2.18	25.3
Strength F_u (N)	4	3.53	10.9
Displacement u_u (m)	2	1.74	21.6

Table 5: *Comparison between experimental and theoretical scale factors, for 1/3 scale*

Characteristic x	Theoretical scale factor $\lambda_x^{(\mathrm{th})}$	Experimental scale factor λ_x	
		Experimental mean $\overline{\lambda_x}$	COV (%)
Elastic stiffness K_e (N/m)	3	3.93	26.7
Strength F_u (N)	9	7.82	10.1
Displacement u_u (m)	3	3.01	17.4

Experimental scale factors have large dispersion. We aim to know if the deviation between theoretical and experimental values are explained by this dispersion, geometrical distortions or phenomena which were not considered.

2.3.1 Elastic stiffness

For the estimated mean of stiffness scale factor, $\mu_{\lambda_{Ke}}$, it is proposed to establish a confidence interval [41]. For that, we assume that experimental mean $\overline{\ln \lambda_{Ke}} = \overline{\ln K_e^{(\mathrm{F})}} - \overline{\ln K_e^{(\mathrm{R})}}$ follows a normal distribution, then the confidence interval for $\mu_{\ln \lambda_{Ke}}$ is obtained by

$$L_i \leq \mu_{\ln \lambda_{Ke}} \leq L_s \tag{7}$$

with

$$L_i = \overline{\ln \lambda_{Ke}} - q\sqrt{\frac{\left(\sigma_{\ln K_e^{(\mathrm{F})}}\right)^2}{n^{(\mathrm{F})}} + \frac{\left(\sigma_{\ln K_e^{(\mathrm{R})}}\right)^2}{n^{(\mathrm{R})}}} \tag{8}$$

and

$$L_s = \overline{\ln \lambda_{Ke}} + q\sqrt{\frac{\left(\sigma_{\ln K_e^{(\mathrm{F})}}\right)^2}{n^{(\mathrm{F})}} + \frac{\left(\sigma_{\ln K_e^{(\mathrm{R})}}\right)^2}{n^{(\mathrm{R})}}} \tag{9}$$

with q *is* the quantile of normal distribution. Finally, we obtained eq (10):

$$\exp\left(L_i + \frac{\left(\sigma_{\ln \lambda_{Ke}}\right)^2}{2}\right) \leq \mu_{\lambda_{Ke}} \leq \exp\left(L_s + \frac{\left(\sigma_{\ln \lambda_{Ke}}\right)^2}{2}\right) \tag{10}$$

with

$$\left(\sigma_{\ln \lambda_{Ke}}\right)^2 = \left(\sigma_{\ln K_e^{(\mathrm{F})}}\right)^2 + \left(\sigma_{\ln K_e^{(\mathrm{R})}}\right)^2 \tag{11}$$

A "risk" parameter α *is defined then* q *is the* $1 - \alpha/2$ *quantile:* α *correspond to the probability that* $\mu_{\lambda_{Ke}}$ *is out of the confidence interval. For* $\alpha = 0.05$, we have $1.87 \leq \mu_{\lambda_{Ke}} \leq 2.72$ for 1/2 reduced scale and $3.39 \leq \mu_{\lambda_{Ke}} \leq 4.88$ for 1/3 reduced scale. For 1/3 reduced scale, it is noticed that $\lambda_{Ke}^{(\mathrm{th})}$ is not included into the confidence interval, in other words the probability that $\lambda_{Ke}^{(\mathrm{th})}$ be equal to $\mu_{\lambda_{Ke}}$ is lower than 0.05, so this hypothesis is rejected. Therefore, differences between theoretical and experimental mean, as displayed on table 5, are significant.

For stiffness K_e, as explained in the end of paragraph 1, edge spacing a_0 and plate's thickness e do not satisfy the similitude relationships. More particularly, λ_{a0} factor experimental value is lower than that required by similitude relationships. In other words, compared to ideal full scale whose scale factors satisfy the similitude relationships, spacing $a_0^{(\mathrm{F})} = \lambda_{a0} a_0^{(\mathrm{R})}$ on full scale is lower, so stiffness $K_e^{(\mathrm{F})}$ increases, then factor $\lambda_{Ke} = K_e^{(\mathrm{F})}/K_e^{(\mathrm{R})}$ is greater, as observed with results displayed on Tables 4 and 5. Indeed, if spacing a_0 decreases, the steel plate's height is lower, so the plate gets less deformed when loaded in height direction, then connection stiffness K_e increases. Otherwise, consequences of λ_e factor on λ_{Ke}, in particular through interaction between bolt and plate, is difficult to evaluate. Also, relative deviation between $\lambda_{Ke}^{(\mathrm{th})}$ and $\overline{\lambda_{Ke}}$ is lower for 1/2 scale than for 1/3 scale, probably because of the relative deviation, between λ_e and λ_{a0} experimental values and those required is lower for 1/2 scale than for 1/3 scale.

Finally, wood heterogeneity, as well as gap and friction between steel and wood, are also distortions which

contribute to deviation between experimental and theoretical scale factor.

2.3.2 Strength

For the estimated mean of strength scale factor, the confidence intervals are $3.30 \leq \mu_{\lambda_{Fu}} \leq 3.81$ for 1/2 reduced scale and $7.34 \leq \mu_{\lambda_{Fu}} \leq 8.39$ for 1/3 reduced scale, with a risk $\alpha = 0.05$. For both 1/2 and 1/3 reduced scales, $\lambda_{Fu}^{(\mathrm{th})}$ value is not included into the confidence interval, so the observed deviations between theoretical $\lambda_{Fu}^{(\mathrm{th})}$ and experimental mean λ_{Fu}, as displayed on tables 4 and 5, are significant.

- Material scale effects (wood and / or bolt) may cause an increase of stress limits at reduced scale, so an increase of $F_u^{(\mathrm{R})}$, therefore a decrease of $\lambda_{Fu} = F_u^{(\mathrm{F})}/F_u^{(\mathrm{R})}$ compared to $\lambda_{Fu}^{(\mathrm{th})}$.

- When edge spacing a_0 is low, it may cause side effect resulting to a reduction of strength F_u. Considering edge spacing a_0 values at different scales, side effect is more important for full scale than for reduced scales. So, side effect may decrease λ_{Fu} compared to $\lambda_{Fu}^{(\mathrm{th})}$.

- Plate's thickness does not satisfy the similitude relationships, this distortion may decrease or increase λ_{Fu} compared to $\lambda_{Fu}^{(\mathrm{th})}$.

Value λ_{Fu} being lower than $\lambda_{Fu}^{(\mathrm{th})}$, we can conclude that causes of discrepancies between λ_{Fu} and $\lambda_{Fu}^{(\mathrm{th})}$ are bolt steel scale effects or side effects or plate's thickness distortion or both. Because of a lack of information about how much material scale effects, side effects and plate's thickness distortion influence λ_{Fu}, it is not possible to conclude more.

If we focus on factor $\lambda_{Fu}^{(1/3\to1/2)}$ which correspond to the ratio between 1/2 and 1/3 reduced scale, because there are probably not side effects at these scales, material scale effects and plate's thickness distortion would be the only phenomena which may impact $\lambda_{Fu}^{(1/3\to1/2)}$. Otherwise, based on results displayed on tables 2 and 3, we obtain $\lambda_{Fu}^{(1/3\to1/2)} = 2.22$ which is very close to the theoretical one $\lambda_{Fu}^{(\mathrm{th},1/3\to1/2)} = \lambda_{Fu}^{(\mathrm{th},1/3)}/\lambda_{Fu}^{(\mathrm{th},1/2)} = 2.25$. So, two hypotheses may be considered: plate's thickness distortion does not impact $\lambda_{Fu}^{(1/3\to1/2)}$ and there are not material scale effects; or plate's thickness distortion impacts $\lambda_{Fu}^{(1/3\to1/2)}$ and there are material scale effects, but these two phenomena compensate. Because of a lack of information about how much material scale effects and plate's thickness distortion influence λ_{Fu}, it is not possible to conclude more.

2.3.3 Load displacement curves

In order to establish similitude laws to the structure, connections load displacement curves at full scale and reduced scale must be similar [6], [42], [43]. Two curves are similar if two values λ_u and λ_F exist, such as, at any reduced scale displacement $u^{(\mathrm{R})}$, $u^{(\mathrm{F})}$ and $F^{(\mathrm{F})}$ can be expressed as following: $u^{(\mathrm{F})} = \lambda_u u^{(\mathrm{R})}, F^{(\mathrm{F})} = \lambda_F F^{(\mathrm{R})}$, with $F^{(\mathrm{F})}$ and $F^{(\mathrm{R})}$ loads corresponding to $u^{(\mathrm{F})}$ and $u^{(\mathrm{R})}$ displacements respectively.

In other words, two curves are similar if the full scale one can be established from the reduced scale one, using two scale factor λ_u and λ_F. Then, scale factors λ_u and λ_F allow to establish the structure similitude laws, but this is not investigated in this article. For curves being similar, their characteristics scale factors have to satisfy the following similitude relationships obtained by DA:

$$\begin{cases} [f_0] = 1 \\ [r_2] = 1 \\ [u_u] = [F_u]/[K_e] \end{cases} \Rightarrow \begin{cases} \lambda_{f0} = 1 \\ \lambda_{r2} = 1 \\ \lambda_{uu} = \lambda_{Fu}/\lambda_{Ke} \end{cases} \tag{12}$$

Then, λ_u and λ_F factors can be obtained by the relationship (13), (14) or (15) :

$$\begin{cases} [u] = [u_u] \\ [F] = [F_u] \end{cases} \Rightarrow \begin{cases} \lambda_u = \lambda_{uu} \\ \lambda_F = \lambda_{Fu} \end{cases} \tag{13}$$

$$\begin{cases} [u] = [F_u]/[K_e] \\ [F] = [F_u] \end{cases} \Rightarrow \begin{cases} \lambda_u = \lambda_{Fu}/\lambda_{Ke} \\ \lambda_F = \lambda_{Fu} \end{cases} \tag{14}$$

$$\begin{cases} [u] = [u_u] \\ [F] = [u_u][K_e] \end{cases} \Rightarrow \begin{cases} \lambda_u = \lambda_{uu} \\ \lambda_F = \lambda_{uu}\lambda_{Ke} \end{cases} \tag{15}$$

Noted that relationships (13) to (15) perfectly match if equation (12) is satisfied.

Considering the obtained model curves (Figures 6, 7 and 8) and their corresponding characteristics scale factors (tables 4 and 5), relationships given by the equation (12) are not satisfied. Therefore, λ_u and λ_F factors given by relationships (13) to (15) are not correct (they do not enable to reproduce the exact full-scale curve from the reduced scale one). However, assume that for some of these relationships, λ_u and λ_F factors enable to reproduce an approximate full-scale curve from the reduced scale one. For each factor given by relationships (13) to (15), an error function is introduced:

$$\varepsilon = \sqrt{\sum_i \varepsilon_i^2} \tag{16}$$

with $\varepsilon_i = \left(F^{(\mathrm{F})} - F^{(\mathrm{F,est})}\right)/F^{(\mathrm{F})}$, $F^{(\mathrm{F})}$ corresponding to $u^{(\mathrm{F})} = \lambda_u u^{(\mathrm{R})}$ and $F^{(\mathrm{F,est})} = \lambda_F F^{(\mathrm{R})}$. ε corresponds to a quadratic mean of the error ε_i for each point of the curves.

Best choices for λ_u and λ_F scale factor could be those which minimize deviation ε. The lower ε is, the more similar are the displacement curves. Then it is so to determine which of these relationships correspond to the smallest deviation ε The Figures 9, 10 and 11 show that, from 1/3 reduced scale, deviations resulting from equations (13) and (14) are relatively close to each other, compared to the one resulting from equation (15). This may be explained by the fact that influence of F_u on curve generally is higher than that of K_e, u_u, f_0 and r_2. So, influence of λ_F factor would be higher than λ_u factor. Furthermore, equations (13) and (14) only differentiate on the least influent factor λ_u, so deviations resulting from these equations are very close from each other. In the same way, equations (14) and (15) only differentiate on the most influent λ_F, so deviations resulting from these equations are very different from each other. More particularly, equation (13) or (14) results to a smaller deviation than equation (15).

Deviations between real and estimated full scale curves can also be investigated through their characteristics such as K_e, F_u and u_u. Comparing real and estimated curves using equation (13) (Figure 9), we notice that F_u and u_u are the same, this is because only F_u and u_u are considered in equation (13). In the same way, comparing real curve and estimated curve using equation (14) (Figure 10), we notice that F_u and K_e are the same, because only F_u and K_e are considered in equation (14). Finally, comparing real curve and estimated curve using equation (15) (Figure 11), we notice that u_u and K_e are the same, because only u_u and K_e are considered in equation (15).

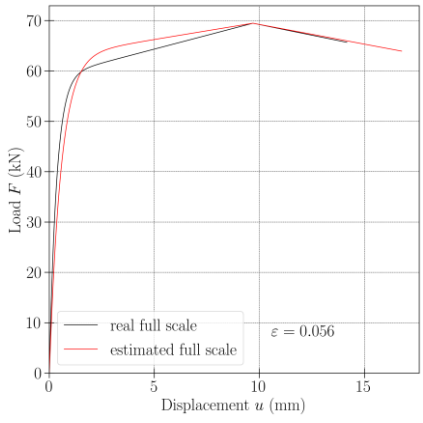

Figure 9: *Full scale curve estimation using equation (13), from 1/3 reduced scale*

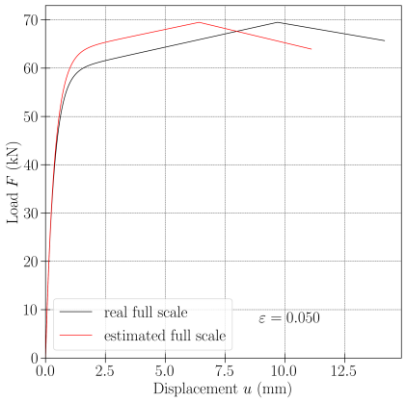

Figure 10: *Full scale curve estimation using equation (14), from 1/3 reduced scale*

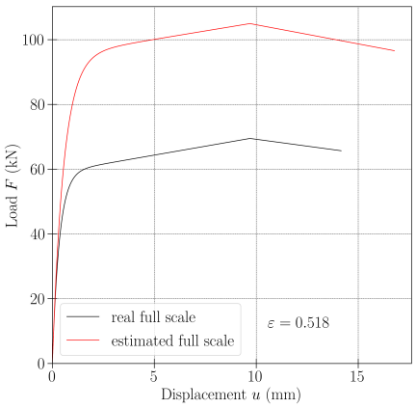

Figure 11: *Full scale curve estimation using equation (15), from 1/3 reduced scale*

3 CONCLUSIONS

These works are the first step of a research program to establish similitude laws to study mid and high-rise timber buildings behaviour.

First, similitude laws were established, using DA method, allowing to estimate the main connections mechanical characteristics. Experiments were carrying on connection in order to determine their characteristics, then deduced experimental scale factors are compared with theoretical ones. Discrepancies were observed between experimental and theoretical scale factors. For stiffness scale factor, these deviations may be explained by the fact that edge spacing and plate's thickness do not satisfy the similitude relationships because of several geometrical "distortions". For strength scale factor, causes of the deviations may be plate's thickness distortion or side effects or material scale effects or both.

Then, characteristics scale factors were used to study connections load displacement curve similitude, in order to establish similitude laws to the structure. This curve similitude between scale and reduced scale was evaluated, and optimal scale factors associated to load displacement curve were investigated. Several potential relations

providing scale factor values were defined, then the best one was determined, based on both 1/2 and 1/3 scales.

Based on connection behaviour similitude evaluation, further studies allowing to establish similitude laws to the structure need to be performed.

ACKNOWLEDGEMENT

The authors gratefully acknowledge the agency for ecological transition (ADEME) and Professional Committee for the Development of French Furniture and Wood Industries (CODIFAB) for financing this work.

REFERENCES

[1] C. P. Coutinho, A. J. Baptista, et J. Dias Rodrigues, « Reduced scale models based on similitude theory: A review up to 2015 », *Engineering Structures*, vol. 119, p. 81-94, juill. 2016, doi: 10.1016/j.engstruct.2016.04.016.

[2] A. Casaburo, G. Petrone, F. Franco, et S. De Rosa, « A Review of Similitude Methods for Structural Engineering », *Applied Mechanics Reviews*, vol. 71, nº 3, p. 030802, mai 2019, doi: 10.1115/1.4043787.

[3] G. J. Simitses et J. Rezaeepazhand, « Structural Similitude and Design of Scaled down Laminated Models », 1993.

[4] S. Kumar, Y. Itoh, K. Saizuka, et T. Usami, « Pseudodynamic Testing of Scaled Models », *Journal of Structural Engineering*, vol. 123, nº 4, p. 524-526, avr. 1997, doi: 10.1061/(ASCE)0733-9445(1997)123:4(524).

[5] H. Yu, W. Zhang, Y. Zhang, et Y. Sun, « Shaking table test and numerical analysis of a 1:12 scale model of a special concentrically braced steel frame with pinned connections », *Earthq. Engin. Engin. Vib.*, vol. 9, nº 1, p. 51-63, mars 2010, doi: 10.1007/s11803-009-8049-0.

[6] P. Moncarz et H. Krawinkler, « Theory and Application of Experimental Model Analysis in Earthquake Engineering », 1981.

[7] J. W. Wissmunn, « Dynamic Stability of Spacevehicles », 1968.

[8] C. J. P. Coutinho, « Structural reduced scale models based on similitude theory », Faculty of Engineering of the University of Porto (FEUP), Porto, 2017.

[9] A. Gauchía, E. Olmeda, M. J. L. Boada, B. L. Boada, et V. Díaz, « Methodology for bus structure torsion stiffness and natural vibration frequency prediction based on a dimensional analysis approach », *Int.J Automot. Technol.*, vol. 15, nº 3, p. 451-461, avr. 2014, doi: 10.1007/s12239-014-0047-1.

[10] Z. Li, F. Ye, et S. Wu, « Design and Experimental Verification of a 1/20 Scale Model of Quayside Container Crane Using Distortion Theory », *Shock and Vibration*, vol. 2019, p. 1-10, août 2019, doi: 10.1155/2019/5893948.

[11] J.-J. Wu, M. P. Cartmell, et A. R. Whittaker, « Prediction of the vibration characteristics of a full-size structure from those of a scale model », *Computers & Structures*, vol. 80, nº 18-19, p. 1461-1472, juill. 2002, doi: 10.1016/S0045-7949(02)00095-0.

[12] Y. Zhu, Y. Wang, Z. Luo, Q. Han, et D. Wang, « Similitude design for the vibration problems of plates and shells: A review », *Front. Mech. Eng.*, vol. 12, nº 2, p. 253-264, juin 2017, doi: 10.1007/s11465-017-0418-1.

[13] C. Adams, J. Bös, E. M. Slomski, et T. Melz, « Scaling laws obtained from a sensitivity analysis and applied to thin vibrating structures », *Mechanical Systems and Signal Processing*, vol. 110, p. 590-610, sept. 2018, doi: 10.1016/j.ymssp.2018.03.032.

[14] B. Zohuri, « Similitude Theory and Applications », in *Dimensional Analysis and Self-Similarity Methods for Engineers and Scientists*, Cham: Springer International Publishing, 2015, p. 93-193.

[15] S. Flores-Bonano, J. Vargas-Martinez, O. M. Suárez, et W. Silva-Araya, « Tortuosity Index Based on Dynamic Mechanical Properties of Polyimide Foam for Aerospace Applications », *Materials*, vol. 12, nº 11, p. 1851, juin 2019, doi: 10.3390/ma12111851.

[16] D. Vassalos, « Physical modelling and similitude of marine structures », *Ocean Engineering*, vol. 26, nº 2, p. 111-123, août 1998, doi: 10.1016/S0029-8018(97)10004-X.

[17] J. Polsinelli et M. L. Kavvas, « A comparison of the modern Lie scaling method to classical scaling techniques », *Hydrol. Earth Syst. Sci.*, vol. 20, nº 7, p. 2669-2678, juill. 2016, doi: 10.5194/hess-20-2669-2016.

[18] Z. Luo, Y. Zhu, X. Zhao, et D. Wang, « Determination method of dynamic distorted scaling laws and applicable structure size intervals of a rotating thin-wall short cylindrical shell », *Proceedings of the Institution of Mechanical Engineers, Part C: Journal of Mechanical Engineering Science*, vol. 229, nº 5, p. 806-817, avr. 2015, doi: 10.1177/0954406214541645.

[19] Z. Luo, Y. Wang, Y. Zhu, X. Zhao, et D. Wang, « The similitude design method of thin-walled annular plates and determination of structural size intervals », *Proceedings of the Institution of Mechanical Engineers, Part C: Journal of Mechanical Engineering Science*, vol. 230, nº 13, p. 2158-2168, août 2016, doi: 10.1177/0954406215592055.

[20] S. Torkamani, A. A. Jafari, et H. M. Navazi, « Scaled down models for free vibration analysis of orthogonally stiffened cylindrical shells using similitude theory », Anchorage, Alaska, USA, 2008, p. 12.

[21] J.-J. Wu, « The complete-similitude scale models for predicting the vibration characteristics of the elastically restrained flat plates subjected to dynamic loads », *Journal of Sound and Vibration*, vol. 268, nº 5, p. 1041-1053, déc. 2003, doi: 10.1016/S0022-460X(03)00303-1.

[22] M. E. Asl, C. Niezrecki, J. Sherwood, et P. Avitabile, « Experimental and theoretical similitude analysis for flexural bending of scaled-down laminated I-beams », *Composite Structures*, vol. 176, p. 812-822, sept. 2017, doi: 10.1016/j.compstruct.2017.06.017.

[23] M. E. Asl, C. Niezrecki, J. Sherwood, et P. Avitabile, « Similitude Analysis of Composite I-Beams with Application to Subcomponent Testing of Wind Turbine Blades », in *Experimental and Applied Mechanics, Volume 4*, C. Sciammarella, J. Considine, et P. Gloeckner, Éd. Cham: Springer International Publishing, 2016, p. 115-126.

[24] M. Eydani Asl, C. Niezrecki, J. Sherwood, et P. Avitabile, « Similitude analysis of thin-walled composite I-beams for subcomponent testing of wind turbine blades », *Wind Engineering*, vol. 41, nº 5, p. 297-312, oct. 2017, doi: 10.1177/0309524X17709924.

[25] M. E. Asl, C. Niezrecki, J. Sherwood, et P. Avitabile, « Scaling and Structural Similarity Under Uncertainty », in *Model Validation and Uncertainty Quantification, Volume 3*, R. Barthorpe, Éd. Cham: Springer International Publishing, 2019, p. 167-174.

[26] M. Hilburger, C. Rose, et J. Starnes, Jr., « Nonlinear analysis and scaling laws for noncircular composite structures subjected to combined loads », *19th AIAA Applied Aerodynamics Conference*, juin 2001, Consulté le: avr. 14, 2020. [En ligne]. Disponible sur: http://arc.aiaa.org/doi/10.2514/6.2001-1335.

[27] S. Balawi, O. Shahid, et M. A. Mulla, « Similitude and Scaling Laws - Static and Dynamic Behaviour Beams and Plates », *Procedia Engineering*, vol. 114, p. 330-337, 2015, doi: 10.1016/j.proeng.2015.08.076.

[28] J. Kasivitamnuay et P. Singhatanadgid, « Scaling laws for static displacement of linearly elastic cracked beam by energy method », *Theoretical and Applied Fracture Mechanics*, vol. 98, p. 157-166, déc. 2018, doi: 10.1016/j.tafmec.2018.10.002.

[29] S. De Rosa, F. Franco, E. Ciappi, et V. Meruane, « Analysis of distorted similitudes for the frequency response of composite plates », *Aerotec. Missili Spaz.*, vol. 95, nº 1, p. 24-31, janv. 2016, doi: 10.1007/BF03404711.

[30] J. D. Barrett, F. Lam, et W. Lau, « Size Effects in Visually Graded Softwood Structural Lumber », *Journal of Materials in Civil Engineering*, vol. 7, nº 1, p. 19-30, févr. 1995, doi: 10.1061/(ASCE)0899-1561(1995)7:1(19).

[31] B. Madsen et A. H. Buchanan, « Size effects in timber explained by a modified weakest link theory », *Can. J. Civ. Eng.*, vol. 13, nº 2, p. 218-232, avr. 1986, doi: 10.1139/l86-030.

[32] B. K. Fryer, R. M. Foster, et M. H. Ramage, « Size effect of large scale timber columns », Seoul, Republic of Korea, 2018, p. 7.

[33] L. Bléron, « Contribution à l'optimisation des performances d'assemblages bois en structure. Analyse de la portance dans les assemblages de type tige. », Université Henri Poincaré, Nancy, 2000.

[34] B. Xu, « Modélisation du comportement mécanique d'assemblages bois avec prise en compte de critères de rupture », Université Blaise Pascal, Clermont-Ferrand, 2009.

[35] J. M. Cabrero et M. Yurrita, « Performance assessment of existing models to predict brittle failure modes of steel-to-timber connections loaded parallel-to-grain with dowel-type fasteners », *Engineering Structures*, vol. 171, p. 895-910, sept. 2018, doi: 10.1016/j.engstruct.2018.03.037.

[36] W. D. Zhang, Z. Luo, X. B. Ge, Y. Q. Zhang, et S. W. Guo, « Determination method of scaling laws based on least square method and applied to rectangular thin plates and rotor-bearing systems », *Mechanics Based Design of Structures and Machines*, p. 1-25, sept. 2019, doi: 10.1080/15397734.2019.1660183.

[37] « Norme d'essai NF EN 26891 ». .

[38] D. Wu, Y. Yamazaki, S. Sawada, et H. Sakata, « Experiment-based numerical simulation of hybrid structure consisting of wooden frame and rigid core », *Engineering Structures*, vol. 182, p. 473-486, mars 2019, doi: 10.1016/j.engstruct.2018.12.085.

[39] B. Folz et A. Filiatrault, « A Computer Program for Cyclic Analysis of Shearwall in Woodframe Structures », 2002.

[40] B. Folz et A. Filiatrault, « A Computer program for seismic analysis of woodframe structures », CUREE, Richmond, Calif., 2002.

[41] B. M. Ayyub et R. H. McCuen, « Probability, Statistics, and Reliability for Engineers and Scientists, Third Edition », 2011.

[42] D.-K. Lee et J.-Y. Cho, « Similitude Law on Material Non-linearity for Seismic Performance Evaluation of RC Columns », *Journal of the Korea Concrete Institute*, vol. 22, nº 3, p. 409-417, juin 2010, doi: 10.4334/JKCI.2010.22.3.409.

[43] J. Park et J.-Y. Cho, « Dynamic Analysis Using Similitude Law Considering Strain Distortion », in *IABSE Symposium Report*, Madrid, sept. 2014, vol. 102, p. 285-292, doi: 10.2749/222137814814027792.